THE UNIVERSITY OF
NEW SOUTH WALES

SCHOOL OF ELECTRICAL ENGINEERING AND TELECOMMUNICATIONS

Transmit Power Minimization for WPT-powered Sustainable IRS - based Multiuser MISO downlink Wireless Systems

Author: Chenyu Gao

Submission Date: 31-July-2020

Master of Engineering science (Electrical)

Abstract:

Greatly thanks to the rapid growth of communication network market as well as dramatically increases of consumers' demands, a tremendous development was experienced by wireless communication network technology. Besides that, due to the ever-increasing environment protection awareness of society, green communication technology caught more attention now.

Simultaneous Wireless information and Power Transfer (SWIPT) as a hotspot of green communication technology research, SWIPT could realize the sustainability of traditional communication devices. Intelligent reflecting surface (IRS) is an innovative technology for enhancing 5G network performance, and this technique is promised for supplying better spectrum and energy efficiency. However, both SWIPT and IRS techniques are all need further optimizing for balancing the quality of service as well as the energy consumption.

Due to that, this paper provides a novel IRS panel which passive reflecting elements are given ability of harvesting wireless power. Further, this paper investigates a multi input single output (MISO) system which assisted by this power harvesting IRS. Additionally, this paper contains the joint study of beamformer of access point, phase shift schedule and harvesting schedule of IRS elements for obtaining lowest transmit power.

Acknowledgement

Foremost, I whish to show my sincere gratitude to my supervisor, Dr. Derrick Kwan Ng for his limitless support for my research and study, and I am so appreciating for his endless encouragement. Due to his supervision and guidance I can comprehend the filed of communication networks and IRS technology.

Also, I would like to thank all people involving in make contribution of the contents of this thesis report.

Contents

Abbreviation

WPT	wireless power transfer
IRS	intelligent reflecting surface
MISO	multiple-input single-output
UDNs	ultra-dense networks
D2D	device-to-device
LTE	Long-Term Evolution
LTE-U	unlicensed spectrum
M-MIMO	massive multiple-input multiple-output
RF	radio frequency
MEMS	micro electromechanical system
AP	access point
AO	alternating optimization
SINR	Signal-to-interference-plus-noise ratio

Chapter 1

Introduction

Benefit by limitless demand of faster network speed, lower latency, and higher quality of service, wireless communication technology experienced a rapid development. 5G communication wireless network was employed now days, 5G network will expand the network traffic band by 100 to 1000 times wider comparing with 4 G technology, and latency will be decreased by less than 1ms. However, in order to realize these characteristics of network, high density of base station deployment as well higher energy consumption is necessary. Due to that, green 5G concept emerged recently. In the future, 6G communication networks the connectivity density will arrive 10^7 $devices/km^2$ [1], nonetheless, battery powered or grid powered network equipment will induce large energy waste. Thus, wireless power transfer (WPT) is a reasonable solution to enhance energy efficient in future communication network system [2]. By the way, this method may eliminate other cost like manually battery replacing and complex grid supply design. Moreover, in reality, harvest power from wireless radio signal is much more solid than capture power from nature, such as, solar or wind, due to the uncertainty of environment disturbing.

In practice, due to the trees and different kinds of constructions obstruction, wireless network performance was limited, thus, intelligent reflecting surface (IRS) technology is proposed for solving this challenge. The basic IRS assisted wireless network is shown below in figure (1). The traditional IRS panel is constituted by plenty of passive reflecting elements, for changing the phase of input signal transmitted from base station antennas and reflecting the signal to specific user. These elements consume very low power for realizing the phase shift controlling. Further, intelligent controlling of phase shifts of every single reflecting element will adapt the real time network channel situation according to the real time update data. Compared with traditional direct transmission system the IRS system can expand the coverage of signals due to the extra reflection. Benefit by these listed perspectives, IRS technology could set up a communication system which have less interference as well as higher efficiency.

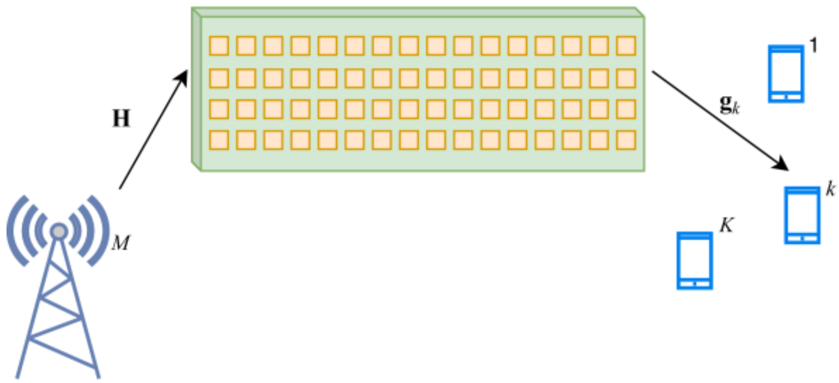

Fig. 1 IRS assisted wireless network

Cited from Basar. E's work in 2019

In general, the consumption of IRS is usually ideally assumed ignorable compared with transmit power and other consumptions in communication networks. However, in practical system the power consumed by IRS is considerable though it is lower than transmit power. Moreover, most of the power consumption of IRS is due to the circuit and diode consuming of reflection elements' reflecting phase controller. And the value of consumption of individual element is related to the bit resolution of each phase shifter [8]. Further, the total consumption of the whole IRS panel depends on the total elements number of IRS panel. Thus, a massive number of reflection elements are employed to enhance network performance.

Besides these hardware limitations, AP transmission organizing method influencing the network performance seriously too. Thus, implement an optimized software program about resource allocation may improve the network performance vastly.

Moreover, inspired by mentioned investigations, this paper offers a WPT powered sustainable IRS based multiuser MISO downlink wireless system, and the IRS reflection elements is based on discrete phase shifters. Further, an innovative IRS panel is proposed, traditional IRS panel's passive elements are replaced by elements could harvest power by utilizing WPT technology for obtaining the sustainability of self-power-supply. Thus, this IRS panel does not need any extra power supply. Except the hardware design, in order to pursue higher energy efficiency performance, a joint optimization is implemented. In this optimization, AP side precoding, phase shift schedule and power harvesting schedule are taken in account to reduce transmit power. However, the system model formulation is a nonconvex optimization problem, thus, in this paper an alternating optimization-based algorithm is employed to search a suboptimal result of this specific problem. The results of this paper show the tradeoff between signal to interference plus noise ratio (SINR) and minimum transmit power to satisfy the smallest number of AP antennas (less equipment cost), as well as, the tradeoff between the number of reflection elements of IRS and minimum transmit power at AP to satisfy the required of minimum SINR.

Chapter 2

Background

5G techniques:

The fifth generation (5G) wireless network is the latest generation wireless communication technology, in present, 5G has already deployed in many areas and countries. As a development and extending of 4G technology, the performance objectives for 5G technology are high sum-rate of information transfer, lessen transfer latency, decreasing energy consumption, reducing operation cost, increasing system capability and massive devices connectivity [1]-[4]. Further, in the lights of currently released data, the information transfer rate could reach the most 10Gbits/s, which is approximate 100 times faster than traditional 4G LTE cellular networks. Besides that, the other significant characteristic of 5G network is dramatically low latency, which means less than 1ms and this number for 4G networks is about 30-70 ms, and this feature will bring revolutions in many industry domains. Moreover, thanks to the tremendously increasing of data transfer rate, the energy consumption of per bit data transfer will be decreased more than 100 times compared with 4G technology. Due to the massive devices' connectivity feature, everything we use could connect to 5G networks. Thus, they can share and analyses data with each other, and this open the new era of IoT.

At present, 5G technology mainly utilize millimeter wave as well as 6GHz frequency band, further, the mainstream technologies which could realize 5G network are listed:

• ultra-dense networks (UDNs) as well as device-to-device (D2D) communications

• millimeter wave (mmWave) technology as well Long-Term Evolution (LTE) in unlicensed spectrum (LTE-U)

• massive multiple-input multiple-output (M-MIMO).

Listed technologies implement 5G networks primarily from different aspects shown below:

• abridging the distance between receiver and transmitter

• promoting the reuse rate of spectrum

• exploiting unused and unlicensed spectrum

• deploying massive number of antennas for optimizing spectral efficiency (SE)

Green 5G and power harvesting:

Recently, sustainable and environment friendly technology philosophy is emerged and accepted by the engineer society, thus, the green 5G communication network concept is promoted. The core of green 5G is increasing energy efficiency as much as possible, due to that, power harvesting technology become the most popular method to realize sustainability.

Moreover, energy could be harvested from several ways, such as, natural renewable resources and radio frequency (RF) resource. In practical, renewable resource energy harvesting method is constraint by plenty of challenges, for example, environment uncertainty, ununiform distribution of resources and low reliability [3]. Due to these disadvantages, more attentions are paid on RF energy harvesting techniques as known as wireless power transfer (WPT) technology [4]. WPT owns some excellent advantages compared with renewable resources, for example, totally controllable power transfer and solid reliability etc. The equipment with WPT ability can transform signals received to energy this device required, and in this way, the sustainability is reached. Further, the signal could be pre-coded and transmitted at AP, which means the RF signal could be separated by information part and power transfer part. And at receiver side, devices could utilize power transfer part to supply the power requirement of itself and decode or re-transmit the information part for its communication function.

WPT technology could promote the 5G network, and on the other hand, 5G network technologies could boost WPT efficiency either. For example, M-MIMO technique and millimeter wave technique can both improve the WPT efficiency by generating optimized beamforming vector, in addition, D2D communication and UDNs could decrease the communication distance of devices then enhance the WPT efficiency. Additionally, passive communication devices could be employed for reducing the power consumption and in this way WPT efficiency would be improved, further, compared with passive devices active devices may introduce more interferences consequently result in network performance decline. Conventionally speaking, interferences occurring in communication are negative, however, in WPT system interferences may utilized as power transfer media thereby increasing the efficiency. Even according to the work of Qingqing Wu et al. (2016), some interferences could be introduced in signals manually and this practice can improve the performance of whole communication system, particularly as the receive device is energy hungry.

Intelligent reflecting surface (IRS):

Be differ from technologies like multiple-input multiple-output (MIMO), collaborate communication and cognitive radio (CR) [6], which devote to optimize the signal processing performance at transceivers, the IRS technology proposed for weakening the impacts due to complex electromagnetic wave propagation circumstances.

In fact, the traditional passive reflecting surface technology appears and be utilized in amount of applications, such as, satellite/ deep-space communication, remote sensing technology and radar system. However, this technology seldom utilized in commercial and civil communication domain. This situation is blame to the passive reflecting structure only equipped fixed phase reflecting surface, thus, this structure could not implement dynamic phase shift during working. Profit from the rapid advancement in science and technology, especially in the domain of micro electromechanical system (MEMS) and materials, intelligent reflecting surface is developed, which means this IRS structure can reflect signals in dynamic phase shifts [7].

Apart from IRS technology, there still have many different technologies applied relevant design philosophy. Such as, backscatter communication, amplified-and-forward (AF) relay, and active intelligent surface applied massive MIMO [5]-[11]. The significant specifications are displayed in the following table (1).

Table 1. *COMPARISON OF IRS WITH OTHER RELATED TECHNOLOGIES*

Technology	Operating mechanism	Duplex	Number of Tx RF chains required	Hardware cost	Energy consumption	Role
IRS	Passive, reflect	Full duplex	0	Low	Low	Helper
Backscatter	Passive, reflect	Full duplex	0	Very low	Very low	Source
MIMO relay	Active, Rx and Tx	Half/ full duplex	N	High	High	Helper
Massive MIMO	Active, Tx/ Rx	Half/ full duplex	N	Very high	Very high	Source/ destination

This table is cited from Q. Wu and R. Zhang's work in 2019.

According to the work by X. Tan et al. (2018) a novel IRS panel is designed and illustrated as figure (2). Based on this structure figure, the reconfigurable reflection patch is constructed, and for each patch the relay switch is designed. In order to alter the phase shift angle, alterable capacitors required to be integrated in every single unit.

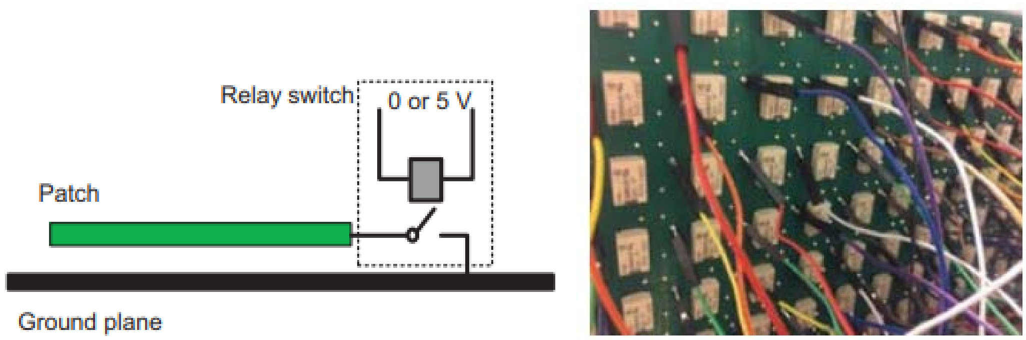

Fig. 2 *The relay switches for reflector units' control.*

Cited from literature of X. Tan et al. (2018).

Figure (3) displays a classic implementation IRS system, there are 3 basic layers are integrated in IRS panel, they are control circuit board, copper backplane and reflection surface[12]. Passive reflecting patches are constructed on a layer of dielectric substrate, and the copper backplane is designed for avoiding the signal leakage, further, the control circuit is designed to realize its responsibility of tuning the amplitude as well the phase according to the command sent by controller. In addition, the microcontroller (FPGA) component in charge of communication and coordination with BS and in order to realize dynamic phase shift [13]-[16].

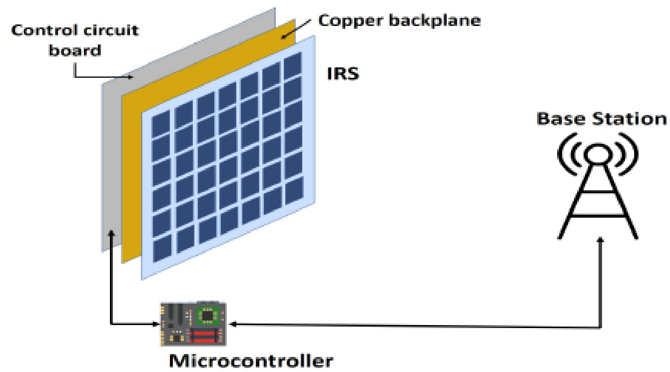

Fig. 3 *typical implementation of an IRS system.*

Cited from Q. Nadeem's literature (2019)

Key Notation

Key Mathematical notations are given in table 1.1 below. The scalars are represented by lowercase letter x, vectors are represented by boldface lowercase letter **x**, matrices are represented by boldface uppercase letter X. $\mathbb{R}^{N\times M}$ signifies $N\times M$ matrices with real entries, and $\mathbb{C}^{N\times M}$ signifies $N\times M$ matrices with complex entries. $\mathbb{H}^{N}$ represents $N\times N$ Hermitian matrices' set. $|\cdot|$ denotes the modulus of a complex-valued scalar, in addition, $\|\cdot\|$ denotes the Euclidean norm of a vector. $(\cdot)^T$, $(\cdot)^H$ represent the transpose and conjugate transpose, respectively. The trace and rank of a matrix is represented as $Tr(\cdot)$ and $Rank(\cdot)$, respectively. $X\succeq 0$ denotes the matrix X is positive semi-definite. $Diag(x)$ denotes a diagonal matrix with its diagonal elements given by vector $x\in\mathbb{C}^{\mathrm{N}\times 1}$. The imaginary unit is represented by j. For a continuous function $f(X)$, $\nabla_X f(\cdot)$ represents the gradient of $f(\cdot)$with respect to matrix X. In addition, $\mathcal{CN}(\mu,\sigma^2)$ denotes a circularly symmetric complex Gaussian distribution, where the μ denotes as mean and σ^2 denotes variance. By the way, the ~ represents the meaning of "distributed as". An $N\times N$ identity matrix is represented by I^N.

Chapter 3

System model

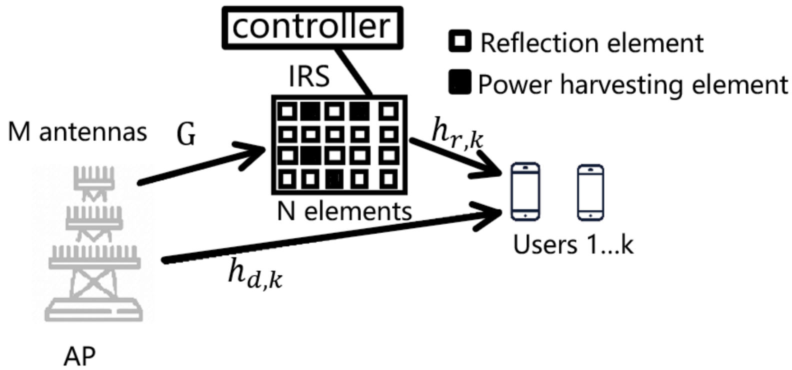

Fig. 4 WPT powered sustainable IRS based multiuser MISO downlink wireless system

A WPT powered sustainable IRS based multiuser MISO system is designed, and as shown in figure (4), the basic system model is illustrated upper. There are $M > 1$ antennas are equipped by the AP in this system and this AP would transmit K individual data streams to K independent users simultaneously. Where, the K users set is denoted as $\mathcal{K} = 1, \ldots, K$. In addition, there are N multifunction IRS elements fabricated on the IRS panel, where N is denoted by a set $\mathcal{N} = 1, \ldots, N$. In this system the reflection schedule matrix is represented as $\Theta = A\Phi$, where $\Phi = diag\left(\beta_1 e^{j\theta_1}, \ldots, \beta_1 e^{j\theta_n}, \ldots, \beta_1 e^{j\theta_N}\right) \in \mathbb{C}^{N\times N}$, and $\theta_n \in [0,2\pi)$ represents the phase shifts, $\beta_n \in [0,1], \forall n \in \mathcal{N}$ is the amplitude coefficient. Further, a diagonal matrix $A = diag(\alpha_1, \ldots, \alpha_n, \ldots, \alpha_N) \in \mathbb{R}^{N\times N}, \forall n \in \mathcal{N}$, moreover, the mode selection factor of IRS is denoted as $\alpha_n \in 0,1$. And as $\alpha_n = 0$ represents IRS element n is working at reflection mode, on the contrary, as $\alpha_n = 1$ represents IRS element n is working at power harvesting mode.

In order to simulate the practical operation, in this paper β_n are all set to a fixed 1, which means the magnitude coefficient is 1 in any situation. Thus, in this system the specific element could only work under reflection mode or power harvesting mode at the same time.

For reasonable complexity of calculation and realistic circuit limitation, a discrete phase shift schedule is designed and employed, thus phase shift interval is quantized like (1).

$$\theta_n \in \mathcal{F} = \{0, \dots, \triangle\theta, \dots, \triangle\theta(B-1)\}, \forall n \in \mathcal{N} \quad (1)$$

Where the phase shifts angles($\triangle\theta = 2\pi/B, B = 2^b$), are stored in set $\mathcal{F}$, besides that b is a given constant number which denoted as bit resolution. Further, the power consumption of each element is denoted as $P_{IRS}(b)$, and this power consumption depends on bit resolution. In working condition, while IRS elements are under reflection mode 100 percent of received waveforms would be reflected, in the other hand, as IRS elements are working under power harvesting mode, the received power which carried by signal waveforms would be totally captured [17]-[26].

In this paper, the channel estimation did not be considered, on account of assuming this system obtain a quasi-static flat fading channel model, further, the channel state information (CSI) is known by AP. In the other words, this system has fixed channel information, thus, only AP side set up as well IRS phase/ mode selection schedules required to be considered. $G \in \mathbb{C}^{N\times M}$ represents the baseband channel from AP to the IRS, $h_{r,k} \in \mathbb{C}^{N\times 1}$ represents the baseband channel from IRS to the kth user, $h_{d,k} \in \mathbb{C}^{M\times 1}$ represents the baseband channel from AP to the kth user. Furthermore, (2) denotes the transmitted signal from AP.

$$x = \sum_{k\in\mathcal{K}} w_k x_k \quad (2)$$

Where $w_k \in \mathbb{C}^{M\times 1}$ on behalf of the AP side precoding vector aim k-th user. In addition, $x_k \sim \mathcal{CN}(0,1), \forall k \in \mathcal{K}$, denotes the data information symbol programmed to send to k-th user. In this IRS system, each user receives the data signal via two disparate links, AP to user link as well AP to IRS to user link. In consequence, the equivalent formula of k-th user's received signal is illustrated as (3)

$$y_k = \left(h_{d,k}^H + h_{r,k}^H A\Phi G\right)\sum_{k\in K} w_k x_k + n_k \quad (3)$$

The background noise occurs at the k-th user is represented by $n_k \sim \mathcal{CN}(0, \sigma_k^2)$, where σ_k^2 is the power noise at k-th user[27]-[30]. Hence, the SINR of received at k-th user is shown below by (4)

$$SINR = \frac{\left|(h_{d,k}^{H}+h_{r,k}^{H}A\Phi G)w_k\right|^2}{\sigma_k^2+\sum_{j\neq k}\left|\left(h_{d,j}^{H}+h_{r,j}^{H}A\Phi G\right)w_j\right|^2} \quad (4)$$

Moreover, γ is raised and it denotes the expected minimum SINR value. Besides previously mentioned parameters, another crucial property is the total received power at power harvesting IRS panel is displayed in (5)

$$y_{EH}(A, w_k) = A_{EH}(Gx + n_a) \quad (5)$$

Where, $n_a \sim \mathcal{CN}(0, \sigma_a^2 I_N)$ represents the receiving thermal noise generated at IRS, in addition σ_a^2 is the receiving noise power at per IRS element. Due to that, the equivalent equation of entirely harvested power of IRS is shown by (6)

$$P_{EH} = \eta_h E(\| A_{EH}(G \sum_{k\in K} w_k x_k + n_a) \|^2) \quad (6)$$

The harvesting power transform efficiency of IRS panel is $\eta_h \in [0,1]$, stand for the convert ratio of received radio signal into electrical energy [31]-[42].

Chapter 4

Problem Formulation

In this study, the aim is to minimalize the transmit power at AP while keeping required SINR at each user and maintaining the power sustainability of IRS. The jointly design is employed, which coordinately take in account with the precoding vector $\{\mathrm{w_k}\}_{\mathrm{k}\in\mathcal{K}}$ at AP , the discrete phase shifter schedule $\{\theta_n\}_{\mathrm{n}\in\mathcal{N}}$ as well the mode selection schedule $\{\alpha_\mathrm{n}\}_{\mathrm{n}\in\mathcal{N}}$.

$$\min_{w_k,\alpha_h,\theta_n} \sum\nolimits_{k\in\kappa} \parallel w_k \parallel^2 \qquad (7)$$

$$\text{s.t. } C1: SINR \geq \gamma,$$

$$C2: \theta_n \in F, \forall n \in N$$

$$C3: \sum\nolimits_{n=1}^{N} P_{IRS}(b) \leq P_{EH},$$

$$C4: \alpha_n \in \{0,1\}, \forall n$$

Thus, the optimization problem formulation could be derived out and illustrated by (7).

Where the objective function on behalf of the sum of transmit power at AP to the whole k users. The constraint C1 makes sure that SINR at each k-th user would not lower than γ, which means the minimum acceptable SINR for each user. The constraint C2 indicates that the phase shift has b-bit resolution, in the other hand, IRS reflection element phase shift angel could only be selected from set $\mathcal{F}$. The constraint C3 points out for maintaining the self-sustainability the power consumption at IRS could not exceed the power harvested harvesting elements of IRS. The constraint C4 represents the mode selection factor and stipulates the IRS elements could not work under harvesting mode and reflection mode simultaneously [38].

For operating the optimization, convexity analyses are necessary. This problem formulation is non-convex, and the non-convexity is caused by several diverse perspectives. For example, the coupling issue between different variables w_k, θ_n and α_n in constraint C1, the discrete issue of phase shift in constraint C2 as well the binary variable problem of α_n in constraint C3 and C4. In conventional method, for searching a globally optimal solution of (7) needs to employ a brute-force searching algorithm, however, the complexity of computation is unaffordable even for a moderate size system. Due to that, as a concession alternating optimization is proposed, further, this is a computationally efficient suboptimal iterative algorithm.

Solution of the optimization problem

A. Problem transformation

For improving the discrete IRS phase shifts design, first the coupling issue of $A\Phi$ in C1 required to be dealt with. For the sake of this, an augmented IRS element mode selection matrix $\tilde{A} = diagram(\tilde{\alpha}) = diag(\tilde{\alpha}_1, \ldots, \tilde{\alpha}_n, \ldots, \tilde{\alpha}_N)$ is proposed. This matrix obtains (B+1) modes, where $\tilde{\alpha}_n \in \tilde{\mathcal{F}} = \{0, e^{j0}, e^{j\triangle\theta}, \ldots, e^{j\triangle\theta(B-1)}\}$ represents the mode options of element n, further, $\tilde{\mathcal{F}}$ denotes the mode options set. Especially, as $\tilde{\alpha}_n = 0$ means element n is under power harvesting mode, otherwise it represents the reflection mode with various phase shifts. Hence, constraint C3 and C4 could be transform as (8) and (9), respectively [40]-[55].

$$C3: \sum_{n=1}^{N} \tilde{\alpha}_n P_{IRS}(b) \leq P_{EH} \qquad (8)$$

$$C4 : \alpha_{\tilde{n}} \in \tilde{F} = \{0, e^{j0}, e^{j\Delta\theta}, \ldots, e^{j\Delta\theta(B-1)}\}, \forall n \quad (9)$$

Moreover, the next nonconvex problem needed to handle is the discrete variable $\tilde{\alpha}_n$ in C3 and C4. Due to that, a new binary mode selection optimization variable is developed, $s_{i,n}, \forall i \in I = \{1, \ldots, \mathrm{B}+1\}, \mathrm{n} \in \mathcal{N}$ further the mode selection matrix is denoted by $S \in \mathbb{R}^{(B+1)\times N}, s_{i,n} \in S$. $s_{i,n} = 1$ means the i-th mode is selected by element number n. As a result of that, the constraint C4 could be augmented as:

$$C4a: \sum_{i\in I} s_{i,n} \leq 1, \forall n \qquad (10)$$

$$C4b: \alpha_{\tilde{n}} = \sum_{i\in I} s_{i,n} f_i, \forall n \qquad (11)$$

$$C4c: s_{i,n} | in\{0,1\}, \forall i, n \qquad (12)$$

The f_i in (11) belones to the set of mode selection indecated in (9). In addition, constraint C3 could be improved by developed C4 , $A_{EH} = diag(s_1)$ where $s_1 = \left[s_{1,1}, \ldots, s_{1,n}, \ldots, s_{1,N}\right]^T$ and it denoted as the first row of mode selection matrix S. Hence, the constraint C3 could be equivalently treansformed to (13).

$$\overline{C3}: (N - \sum_{n-1}^{N} s_{1,n})P_{IRS}(b) \leq \eta_h(\sum_{k\in K} Tr(Gw_k w_k^H G^H diag(s_1) + \sigma_a^2 \sum_{n=1}^{N} s_{1,n})) \quad (13)$$

According to the (13), in order to realize the expected self-sustainability of IRS system, a partial of IRS elements are selected to harvest power, meanwhile, the rest of elements are adjusted to specificate phase shifts for enabling the reflecting function. Therfore, the optimization formulation could be rewirten as (14)

$$\min_{w_k, \tilde{\alpha}_n, S} \sum_{k\in K} \| w_k \|^2 \quad (14)$$

t.s. $C1: SINR \geq \gamma,$

$$\overline{C3}: (N - \sum_{n-1}^{N} s_{1,n})P_{IRS}(b) \leq \eta_h(\sum_{k\in K} Tr(Gw_k w_k^H G^H diag(s_1) + \sigma_a^2 \sum_{n=1}^{N} s_{1,n}))$$

$C4a: \sum_{i\in I} s_{i,n} \leq 1, \forall n$

$C4b: \tilde{\alpha}_n = \sum_{i\in I} s_{i,n} f_i, \forall n$

$C4c: s_{i,n} | in\{0,1\}, \forall i, n$

In the following, this paper will concentrate of solving this optimization problem (14). This formulation is still nonconvex, nonetheless, this transformed formulation provide an ability to implement the alternating optimization (AO) algorithm for acquiring a reasonable suboptimal solution. In practice, this AO algorithm settles the coupling issue about variables w_k and $\{S, \tilde{\alpha}_n, \forall n\}$ by separating them into two different subproblems [54]-[60]. Then, in each subproblem one of the variables w_k and $\{S, \tilde{\alpha}_n, \forall n\}$ is defined as a fixed solution in solving each subproblem.

B. subproblem1: optimization of precoding at the AP

In this part, the aim is to optimize the transmit beamforming vector w_k, by utilizing a set of given fixed feasible point $\{S^{cont}, \tilde{\alpha}_n^{cont}, \forall n\}$, where S^{cont} and $\tilde{\alpha}_n^{cont}$ represent IRS element mode selection fixed value binary matrix and n-th element mode selection fixed

$$\min_{w_k} \sum_{k\in\kappa} Tr(W_k) \qquad (15)$$

$$C1: \frac{Tr(W_k M_k)}{\sigma_k^2 + \sum_{i\neq k} Tr(W_j M_k)} \geq \gamma,$$

$$\overline{C3}: (N - \sum_{n-1}^{N} s_{1,n}) P_{IRS}(b) \leq \eta_h (\sum_{k\in K} Tr(G w_k w_k^H G^H diag(s_1) + \sigma_a^2 \sum_{n=1}^{N} s_{1,n}))$$

$$C5: W_k \succeq 0, \forall k,$$

$$C6: Rank(W_k) \leq 1, \forall k$$

value , respectively. Thus, the subproblem could be written as (15)

By defining $W_k \triangleq w_k w_k^H$ and $M_K = m_k m_k^H, m_k = h_{d,k} + G^H \tilde{A}^H h_{r,k}$. Further, constraints C5, C6 and $W_k \in \mathbb{H}^M$ are emerged to guarantee that $W_k = w_k w_k^H$ still remained after optimizing operation.

For this subproblem formulation, the constraint C6 is the only non-convex, in the sake of avoiding this issue, semidefinite relaxation (SDR) technique is adopted and due to that the rank constraint (C6) is discarded. Hence, the optimization problem resulted is

$$\min_{w_k} \sum_{k\in K} Tr(W_k) \qquad (16)$$

$$C1: \frac{Tr(W_k M_k)}{\sigma_k^2 + \sum_{i\neq k} Tr(W_j M_k)} \geq \gamma,$$

$$\overline{C3}: (N - \sum_{n-1}^{N} s_{1,n}) P_{IRS}(b) \leq \eta_h (\sum_{k\in K} Tr(G w_k w_k^H G^H diag(s_1) + \sigma_a^2 \sum_{n=1}^{N} s_{1,n}))$$

$$C5: W_k \succeq 0, \forall k$$

illustrated as (16).

For now, this subproblem (16) is a convex problem that could be solved by some kinds of standar convex program solvers. Moreover, in the following theorem, the tightness of the employed SDR has been discussed.

Theorem 1. *With* $P_{MAX} > 0$ *and in case of (1) is feasible, a rank-one solution of (16) will always be satisfied.*

Proof: the detiled proof will be demonstrated in appendix, and at here a brief structure of the proof [55]-[60]. By analyzing the Karuch-Kuhn-Tucker (KKT) conditions of problem (16), we could confirm there must exist a rank-one solution W_k in order to obtain a boundedd dual problem solution of (16). Moreover, we could derive out a rank-on solution by utilizing the dual variables of the dual problem of (16).

Due to the problem (16) is convex, we could iteratively update the feasible solution W_k by figuring the subproblem of (16) in $t^{(1)}$ iteration. The employed convex problem

Algorithm 1: Iterative AP precoder design

1: Initialize the maximum number of iterations $t_{max}^{(1)}$, and initialize the initial iteration index $t^{(1)} = 0$, as well given constants $\{S^{cont}, \tilde{\alpha}_n^{cont}, \forall n\}$, and the target optimizing variable $W_k^{t(1)}$:

2. **repeat** {Main loop}

3. solve problem (16) with given $W_k^{t(1)}$ and $\{S^{cont}, \tilde{\alpha}_n^{cont}, \forall n\}$, to acquire $W_k^{t(1)+1}$;

4. set $t^{(1)} = t^{(1)} + 1$:

5. **until** convergence or $t^{(1)} = t_{max}^{(1)}$

solving algorithm is shown in **Algorithm 1**.

C. sub-problem 2: optimization of IRS mode selection and phase shifts

For this sub-problem, we demand to optimize the mode selection matrix $S = \{s_{i,n}, \forall i, n\}$ at meanwhile the transmit precoder vector $\{w_k^{cont}, \forall k\}$ is fixed. Firstly, the binary variable $s_{i,n}$ need to be tackled, thus the constraint C4c could be equivalently rewritten to the below two constraints, (17) and (18) respectively.

$$\overline{C4c}: s_{i,n} - s_{i,n}^2 \leq 0, \forall i, n \quad (17)$$

$$C4d: 0 \leq s_{i,n} \leq 1, \forall i, n \quad (18)$$

At here, the $s_{i,n}, \forall i, n$ is transformed into continuous variables. For easier presentation, let $L_k = diag(h_{r,k}^H)G$. Applying $h_{r,k}^H \bar{A} G = v^H L_k$ where $v = [\widetilde{\alpha_1}, \ldots, \widetilde{\alpha_n}, \ldots, \widetilde{\alpha_N}]^H$, then we acquire $\left|h_{d,k}w_k + G^H \tilde{A}^H h_{r,k} w_k\right|^2 = |h_{d,k}^H w_k + v^H L_K w_k|^2$. Thus, the sub-problem 2

$$\min_{S, v, \varepsilon_k, \iota_k} \sum_{k \in K} Tr(W_k^{cont}) \qquad (19)$$

$$\boldsymbol{s.t.}\, C1: \frac{\varepsilon_k}{\sigma_k^2 + \iota_k} \leq \gamma, \forall k,$$

$$C3: \sum_{n=1}^{N} \tilde{\alpha}_n P_{IRS}(b) \leq P_{EH}$$

$$C4a: \sum_{i \in I} s_{i,n} \leq 1, \forall n$$

$$C4b: \tilde{\alpha}_n = \sum_{i \in I} s_{i,n} f_i, \forall n$$

$$\overline{C4c}: s_{i,n} - s_{i,n}^2 \leq 0, \forall i, n$$

$$C4d: 0 \leq s_{i,n} \leq 1, \forall i, n$$

$$C7: \varepsilon_k \leq |h_{d,k}^H + v^H L_k w_k|, \forall k,$$

$$C8: \iota_k \geq \sum_{j \neq k} |h_{d,k}^H + v^H L_k w_k|, \forall k,$$

could be transformed as (19).

Where, $\varepsilon_k = |h_{d,k}^H + v^H L_k w_k|, \forall k$, and $\iota_k = \sum_{j \neq k} |h_{d,k}^H + v^H L_k w_k|, \forall k$, are two slack optimization variables. In practical, the inequality constraints C7 and C8 are always contentmented equality at the optimal solution of (19). It can be observed that this sub-problem (19) is convex, thus a standar convex solver could be utilized for searching and updating the feasible solution $\{S, v, \varepsilon_k, \iota_k\}$. Further, the proposed algorithm for solving (19) is displayed in **Algoritm 2**, meanwhile, the orgnized overall solving algorithm is shown in **Algoritm 3** [61]-[65]. And the algoritm 3 summarizes and solves the two sub-problems in (16) anmd (19) iteratively. Further, some issues require to be declared, the convergence of algoritm 3 to a suboptimal solution of (7), in order to satisfy the reasonable computational complexity.

Algorithm 2: Iterative IRS mode selection schedule and phase shift schedule design

1: Initialize the maximum number of iterations $t_{max}^{(2)}$, and initialize the initial iteration index $t^{(2)} = 0$.

2. Given $\{W_k^{cont}, \forall k\}$. Initialize variables $\{s_{i,n}^{t(2)}, \forall i, n\}$, $\{v_n^{t(2)} = \sum_{i \in \mathcal{F}} s_{i,n}^{t(2)} f_i^*, \forall n\}$, $\{\iota_k^{t(2)}, \forall k, j\}$ *and* $\{\varepsilon_k^{t(2)}, \forall k\}$.

3. **repeat** {Main loop}

4. solve problem (19) with given $\{W_k^{cont}\}$ $\{v_n^{t(2)}, \forall n\}$, $\{\iota_k^{t(2)}, \forall k, j\}$ and $\{\varepsilon_k^{t(2)}, \forall k\}$. And obtain$\{s_{i,n}^{t(2)}, \forall i, n\}$, $\{v_n^{t(2)}, \forall n\}$, $\{\iota_k^{t(2)}, \forall k, j\}$ and $\{\varepsilon_k^{t(2)}, \forall k\}$.;

5. set $t^{(2)} = t^{(2)+1}$;

5. **until** convergence or $t^{(2)} = t_{max}^{(2)}$

Algorithm 3: Alternating optimization algorithm

1: Initialize the maximum number of iterations $t_{max}^{(3)}$, and initialize the initial iteration index $t^{(3)} = 0$.

2.Variables $\{w_k^{cont}, \forall k\}$ and $\{s_{i,n}^{t(3)}, \tilde{\alpha}_n^{t(3)}, \forall n\}$.

3. **repeat** {Main loop}

4. Obtain $W_k^{t(3)+1}$ by algorithm 1 with $W_k^{t(3)}$, $\{s_{i,n}^{t(3)}, \forall n, i\}$ and $\{\tilde{\alpha}_n^{t(3)}, \forall n\}$.

5. Obtain $\{s_{i,n}^{t(3)+1}, \forall i, n\}$, $\{v_n^{t(3)+1}, \forall n\}$ by algorithm 2 with given $W_k^{t(3)+1}$ and $\{v_n^{t(3)}, \forall n\}$;

6. Update $\{\tilde{\alpha}_n^{t(3)+1}, \forall n\}$ and $\{v_n^{t(3)+1}, \forall n\}$;

7. Set $t^{(3)} = t^{(3)+1}$:

5. **until** convergence or $t^{(3)} = t_{max}^{(3)}$

Chapter 5

Numerical results

In this section, I analyze the communication system performance of the suggested self-sustainable IRS scheme via software simulation. The overall system setting is demonstrated in figure (5).

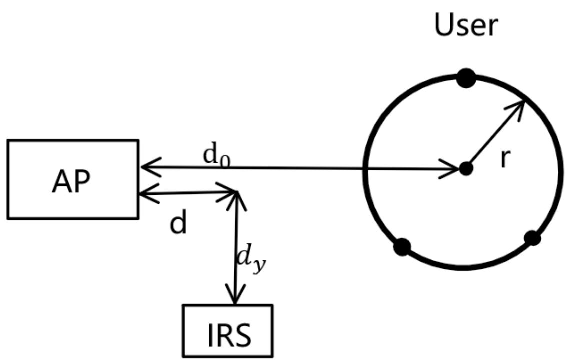

Figure (5) simulation system setup

According to this picture, the users are distributed in a circular domain randomly and this region has a center point and 1m radius represented by r. The distance between AP and the center point of users' distribution arear is set as $d_0 = 60m$. The IRS panel is located between AP as well user arear center point with an extra vertical distance $d_y = 1m$. Further the horizontal distance from the AP to center point is noted as dm. There are M antennas are constructed in AP with a uniform linear array. N elements are fabricated on IRS panel and distributed uniformly, in addition, the user number is set to $K = 2$. The path loss needed to be considered and this value is dependent on the distance, due to that, a reasonable distance-dependent path loss model is employed. The AP transmit antenna gains and IRS receive antenna gains are uniformly decided as 10 dBi, moreover, each user's antenna gain is set as 0 dBi. In addition, the reference distance of the path loss model is 10 meters. The path loss exponents of AP-user link are confirmed as $\alpha_{AU} = 3.6$, due to the by contrast long distance and random scattering of AP-user link. Besides that, we set the AP-IRS and IRS-user link path loss exponents as $\alpha_{AI} = \alpha_{IU} = 2.2$, because IRS is always located for constructing a line-of-sight (LoS) channel with AP.

Furthermore, the system bandwidth is 200kHz and the carrier center frequency is confirmed by 750MHz. In this system, the small-scale fading coefficients are produced as independent and identically distributed (i.i.d.) Rican random variables with Rician factors. Thus, for AP-user link, AP-IRS link and IRS-user link the fading coefficients are $\beta_{AU} = 0$, $\beta_{AI} = 2$ and $\beta_{IU} = 0$, respectively. In addition, the signal processing noise occurs at each receiver is primarily induced by thermal noise and quantization noise. In particularly, in this system a 12-bits uniform quantizer is employed to quantize the received information at every user receiver. Thus, the thermal noise power is -110 dBm and quantization noise power is -47 dBm for every individual user. Other significant parameters and upper mentioned factors are summarized in the following table (2) for easy searching.

Table (2) *significant parameters of system simulation*

Parameter name	value
Antenna gains of AP and IRS	10 dBi
Antenna gains of users	0 dBi
System bandwidth	200 kHz
Carrier center frequency	470 MHz
Path loss exponent	$\alpha_{AU} = 3.6$, $\alpha_{AI} = \alpha_{IU} = 2.2$
Fading coefficients	$\beta_{AU} = 0$, $\beta_{AI} = 2$ and $\beta_{IU} = 0$,
Phase shift bit resolution	b=3
Thermal noise power	-110 dBm
Quantization noise power	-47 dBm
Required minimum SINR	$\gamma = 21\ dB$
Power consumption of each element with b bit resolution	$P_{IRS}(b = 3) = 1dBm$
Power harvesting efficiency of IRS	$\eta_h = 0.8$

For comparison, I set up two different simulating schedules. First, elements quantity located on the IRS panel is set as a variable for studying the relationship between average total transmit power and IRS elements quantity. Then, there are three specific SINR is given for evaluating the system performance under different SINR requirements and meanwhile the AP antennas quantity is fixed as 8. Secondly, the variable is minimum required SINR, along with the changing of required SINR the average total transmit power is changed and the connection of them is observable. Further, I set three groups for simulation according to diverse AP antenna numbers and with same IRS elements as 100.

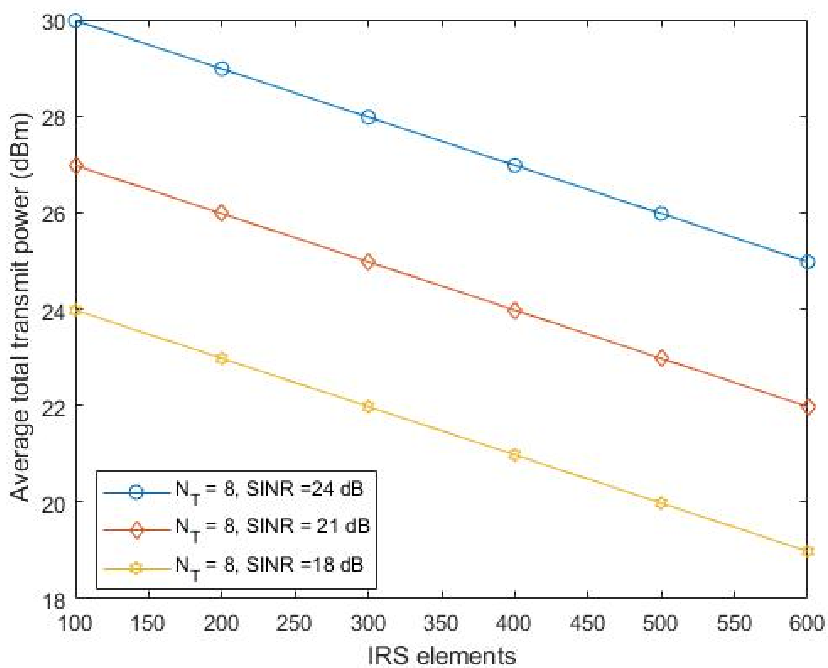

Figure (6) average total transmit power verse IRS elements

With different minimum required SINR

According to figure (6), for same SINR an evident decline occurred along with the increasing of IRS elements on per IRS panel, the value decreased from 24 dBm towards to around 19 dBm as SINR is fixed as 18 dB. And this dropped value for SINR= 21 dB and 24 dB is from 27dBm to 22dBm and from 30dBm to 25dBm, respectively. There is a linear relationship between IRS elements as well total transmit power, besides that, through the observation, the transmit power improved 3dBm due to the SINR increased 3 dB. In conclusion, with the increasing of the IRS elements the transmit performance is enhanced and meanwhile if lower SINR is accepted the power consumption would be declined either.

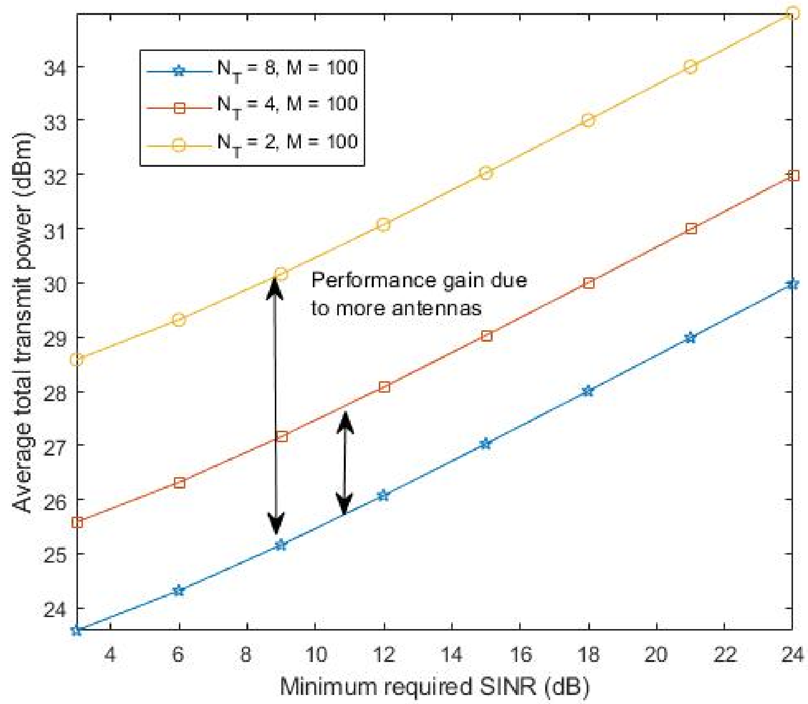

Figure (6) average total transmit power verse minimum required SINR

With different number of AP antennas

In figure (6), the tendency of average total transmit power is boosting when minimum required SINR is increased. However, unlike the condition in figure (5), the total transmit power experiences a nonlinear growing, and the growing's acceleration is keeping genteelly increasing. Further, according to this figure, as AP antenna number be improved, the transmit power is significantly decreased, which means the power efficiency is improved. Moreover, the performance gain is marked on this figure, we could discover that as the number of AP antenna increased from 2 to 4 then to 8 the average declined transmit power is about 3 dBm and 2 dBm, respectively. In conclusion, the AP antennas' quantity influences the transmit power performance significantly but as the number going bigger the performance gain would shrink instead.

Conclusion

The eventually objective is to design and propose a computational friendly WPT powered sustainable IRS based multiuser MISO downlink wireless system. During the research period, various of studies could contribute to implement this system model were conducted. The focus of this study is to enhance the power efficiency of the traditional 5G wireless communication net works, and in view of the practical implementation IRS technology is selected from several related technologies mentioned in table (1).

For better energy efficiency performance, a further research is conducted. WPT is a popular technology which owns plenty of advantages could improve the utilization of RF signals. Due to that, WPT is employed on this IRS model, and a WPT powered self-sustainable IRS panel is proposed. By utilizing the power harvesting elements constructed on the IRS panel, vast of wasted power is harvested, further, the communication performance is boosted either by declining the interferences due to the introduction of WPT technique.

Furthermore, in order to assist this system working under better mode, a jointly design of beamform precoder at the AP and the power harvesting schedule and the phase shift schedule is emerged. Due to the non-convexity of this jointly design model, several convex optimization methods are employed, such as, alternating optimization and semidefinite relaxation (SDR) techniques. Then, a suboptimal solution is obtained by introducing these algorithms.

Moreover, the simulation model and results are demonstrated. According to the results, the relationships between average total transmit power and minimum required SINR and AP antenna quantity and IRS located element quantity are all unveiled.

At last, due to all the works mentioned, an optimized IRS system equipped with power harvesting elements is eventually set up.

Appendix

As mentioned in the optimal solution part, in order to eliminate the nonconvex rank one constraint in (15), the SDR technique is utilized. For testifying the optimized problem (16) is convex and feasible, the slater's constraint required to be satisfied and the strong duality holds need to be ensured. Thus, the strong duality could be defined by construct a LaGrange dual function, moreover, the optimal value of the dual problem is simultaneously equal to the primal problem's optimal value [66]-[69].].

For the sake of proving the SDR is tight, KKT condition of optimization problem is evaluated. First of all, the Lagrangian function is derived (20):

$$L(W_k, \lambda_1, \lambda_2, \lambda_3) = \sum_{k\in K} Tr(W_k) + \lambda_1(\gamma(\sigma_k^2 + \sum_{i\neq k} Tr(W_j M_k)) - Tr(W_k M_k)) + \lambda_2((N - \sum_{n-1}^{N} s_{1,n})P_{IRS}(b) - \eta_h(\sum_{k\in K} Tr(G w_k w_k^H G^H diag(s_1) + \sigma_a^2 \sum_{n=1}^{N} s_{1,n}))) + \lambda_3 Tr(-W_k) - Tr(YW_k) \quad (20)$$

Where Y, λ_1, λ_2 and $\lambda_3$are dual variables associate with the constraints C6, C1, $\overline{C3}$ and C5 of the optimization problem respectively. In addition, the Lagrangian function is used to find the dual problem of the given primal problem (15). Due to that, the dual problem can be expressed as (21):

$$\max_{Y,\lambda_1,\lambda_2,\lambda_3} \inf_{W_k,\tau\in H^T} L \quad (21)$$

And now, concentrating on the KKT conditions:

$$Y \succeq O, \lambda_1, \lambda_2, \lambda_3 \geq 0 \quad (22)$$

YW=0, (23)

Y=-H+B (24)

For equation (24) is derived by taking the derivative of the Lagrangian function with respect to W_k, moreover $B = -\lambda_1 M_k - \lambda_2 \eta_h (Gdiag(s_1)) + \lambda_3(-I)$. Where, the equation (23) denotes a complementary slackness property. Due to that, if $Rank(Y) \geq N - T - 1$ could be proved, then the beamforming matrix W is a rank-one or zero matrix. Assuming that the B is a positive semi-definte matrix, then tere is at least one zero enginvalue and an associated enginvextor is exist and denoted as v. Further, we creat a matrix $V = vv^H$ without harming the generality. By mulitplying (24) from both side using v and v^H than operating the trace operation, then (25) gaind.

$$Tr(YV) = -Tr(HV) + Tr(BV) = -Tr(HV) \quad (25)$$

Due to H and $Gdiag(s_1)$ as well M_k are all independent, we have strictly $Tr(HV) > 0$, which falsify the $Tr(HV) > 0$. Hence, matrix B is positive definite matrix, and $Rank(B) = N_T$. Furthermore, according to the Lemma 1, (26) is illustrated.

Lemma 1. Let A and B be two matrices with same dimension. The inequality of matrix $Rank(A + B) \geq Rank(A) - Rank(B)$ holds.

$$Rank(Y) = Rank(-Y) = Rank(-B + H) \geq Rank(-B) - Rank(H) = NT - 1 \quad (26)$$

At last as $Rank(Y) \geq N_T - 1$, the SDR technique is proofed reasonable in problem (15).

References

1. J. G. Andrews, S. Buzzi, W. Choi, S. V. Hanly, A. Lozano, A. C. Soong, and J. C. Zhang, “What will 5G be?” IEEE J. Sel. Areas Commun., vol. 32, no. 6, pp. 1065?1082, Jun. 2014.
2. Q. Wu, G. Y. Li, W. Chen, D. W. K. Ng and R. Schober, "An Overview of Sustainable Green 5G Networks," in IEEE Wireless Communications, vol. 24, no. 4, pp. 72-80, Aug. 2017.
3. Y. Chen, S. Zhang, S. Xu, and G. Y. Li, “Fundamental trade-offs on green wireless networks,” IEEE Commun. Mag., vol. 49, no. 6, pp. 30?37, Jun. 2011.
4. Q. Wu, G. Y. Li, W. Chen, and D. W. K. Ng, “Energy-efficient small cell with spectrum-power trading,” arXiv preprint arXiv:1608.03178, 2016.
5. R. Zhang and C. K. Ho, "MIMO Broadcasting for Simultaneous Wireless Information and Power Transfer," in IEEE Transactions on Wireless Communications, vol. 12, no. 5, pp. 1989-2001, May 2013.
6. S. Timotheou and I. Krikidis, “Joint Information and Energy Transfer in the Spatial Domain with Channel Estimation Error,” Proc. IEEE Online Conf. Green Commun., Oct. 2013, pp. 115-120.
7. Z. Hasan, G. Bansal, E. Hossain, and V. Bhargava, “Energy-Efficien Power Allocation in OFDM-Based Cognitive Radio Systems: A Risk-Return Model,” IEEE Trans. Wireless Commun., vol. 8, pp. 6078–6088, Dec. 2009.
8. G. Miao, N. Himayat, and G. Li, “Energy-Efficient Link Adaptation in Frequency-Selective Channels,” IEEE Trans. Commun., vol. 58, pp. 545–554, Feb. 2010.

9. D. Ng, E. Lo, and R. Schober, “Energy-Efficient Resource Allocation in OFDMA Systems with Hybrid Energy Harvesting Base Station,” IEEE Trans. Wireless Commun., vol. 12, pp. 3412–3427, Jul. 2013.
10. S. Leng, D. W. K. Ng, N. Zlatanov and R. Schober, "Multi-objective beamforming for energy-efficient SWIPT systems," 2016 International Conference on Computing, Networking and Communications (ICNC), Kauai, HI, 2016, pp. 1-7.
11. Q. Wu and R. Zhang, "Intelligent Reflecting Surface Enhanced Wireless Network via Joint Active and Passive Beamforming," in IEEE Transactions on Wireless Communications, vol. 18, no. 11, pp. 5394-5409, Nov. 2019.
12. X. Tan, Z. Sun, D. Koutsonikolas and J. M. Jornet, "Enabling Indoor Mobile Millimeter-wave Networks Based on Smart Reflect-arrays," IEEE INFOCOM 2018 - IEEE Conference on Computer Communications, Honolulu, HI, 2018, pp. 270-278.
13. Nadeem Q U A, Kammoun A, Chaaban A, et al, “Intelligent Reflecting Surface Assisted Wireless Communication: Modeling and Channel Estimation”, Nadeem 2019 intelligent, 2019.
14. Q. Wu and R. Zhang, "Intelligent Reflecting Surface Enhanced Wireless Network: Joint Active and Passive Beamforming Design," 2018 IEEE Global Communications Conference (GLOBECOM), Abu Dhabi, United Arab Emirates, 2018, pp. 1-6.
15. B. Clerckx, R. Zhang, R. Schober, D. W. K. Ng, D. I. Kim, and H. V. Poor, “Fundamentals of wireless information and power transfer: From RF energy harvester models to signal and system designs,” IEEE J. Select. Areas Commun., vol. 37, no. 1, pp. 4–33, Sep. 2018.

16. H. Fu, S. Feng, W. Tang and D. W. K. Ng, "Robust Secure Resource Allocation for Downlink Two-User MISO Rate-Splitting Systems," *2020 IEEE International Conference on Communications Workshops (ICC Workshops)*, Dublin, Ireland, 2020, pp. 1-7.
17. Y. Cai, Z. Wei, S. Hu, D. W. K. Ng and J. Yuan, "Resource Allocation for Power-Efficient IRS-Assisted UAV Communications," *2020 IEEE International Conference on Communications Workshops (ICC Workshops)*, Dublin, Ireland, 2020, pp. 1-7.
18. C. Wang, Z. Li, J. Shi, J. Si and D. W. K. Ng, "Physical Layer Security of Vehicular Networks: A Stochastic Geometry Approach," *2020 IEEE International Conference on Communications Workshops (ICC Workshops)*, Dublin, Ireland, 2020, pp. 1-7.
19. M. Letafati, A. Kuhestani, D. W. K. Ng and H. Behroozi, "A New Frequency Hopping-Aided Secure Communication in the Presence of an Adversary Jammer and an Untrusted Relay," *2020 IEEE International Conference on Communications Workshops (ICC Workshops)*, Dublin, Ireland, 2020, pp. 1-7.
20. W. Yuan, C. Liu, F. Liu, S. Li and D. W. K. Ng, "Learning-based Predictive Beamforming for UAV Communications with Jittering," in *IEEE Wireless Communications Letters*.
21. J. Liu, K. Xiong, D. W. K. Ng, P. Fan, Z. Zhong and K. B. Letaief, "Max-Min Energy Balance in Wireless-Powered Hierarchical Fog-Cloud Computing Networks," in *IEEE Transactions on Wireless Communications*.
22. M. Letafati, A. Kuhestani, H. Behroozi and D. W. K. Ng, "Jamming-Resilient Frequency Hopping-Aided Secure Communication for Internet-of-Things in the Presence of an Untrusted Relay," in *IEEE Transactions on Wireless Communications*.

23. Basar E, Di Renzo M, De Rosny J, et al. Wireless communications through reconfigurable intelligent surfaces[J]. IEEE Access, 2019, 7: 116753-116773.
24. J. Zhang, J. Han, L. Xiang, D. W. K. Ng, M. Chen and M. Jo, "On the Performance of LTE/Wi-Fi Dual-Mode Uplink Transmission: Connection Probability versus Energy Efficiency," in *IEEE Transactions on Vehicular Technology*.
25. Y. Ma, N. Wu, W. Yuan, D. W. K. Ng and L. Hanzo, "Joint Channel Estimation and Equalization for Index-Modulated Spectrally Efficient Frequency Division Multiplexing Systems," in *IEEE Transactions on Communications*.
26. X. Yu, D. Xu, Y. Sun, D. W. K. Ng and R. Schober, "Robust and Secure Wireless Communications via Intelligent Reflecting Surfaces," in *IEEE Journal on Selected Areas in Communications*.
27. J. Liu, K. Xiong, Y. Lu, D. W. K. Ng, Z. Zhong and Z. Han, "Energy Efficiency in Secure IRS-Aided SWIPT," in *IEEE Wireless Communications Letters*.
28. A. Khalili and D. W. K. Ng, "Energy and Spectral Efficiency Tradeoff in OFDMA Networks via Antenna Selection Strategy," *2020 IEEE Wireless Communications and Networking Conference (WCNC)*, Seoul, Korea (South), 2020, pp. 1-6.
29. M. Robat Mili, A. Khalili, n. mokari, S. Wittevrongel, D. W. K. Ng and H. Steendam, "Tradeoff Between Ergodic Energy Efficiency and Spectral Efficiency in D2D Communications Under Rician Fading Channel," in *IEEE Transactions on Vehicular Technology*.
30. J. Zhang, E. Björnson, M. Matthaiou, D. W. K. Ng, H. Yang and D. J. Love, "Prospective Multiple Antenna Technologies for Beyond 5G," in *IEEE Journal on Selected Areas in Communications*.

31. J. Zhang, E. Björnson, M. Matthaiou, D. W. K. Ng, H. Yang and D. J. Love, "Guest Editorial Special Issue on Multiple Antenna Technologies for Beyond 5G-Part II," in *IEEE Journal on Selected Areas in Communications*.
32. C. Ouyang, S. Wu, C. Jiang, D. W. K. Ng and H. Yang, "Secrecy Performance for Finite-Alphabet Inputs Over Fluctuating Two-Ray Channels in FDA Communications," in *IEEE Wireless Communications Letters*.
33. S. Li, W. Yuan, J. Yuan, B. Bai, D. W. K. Ng and L. Hanzo, "Time-Domain vs. Frequency-Domain Equalization for FTN Signaling," in *IEEE Transactions on Vehicular Technology*.
34. G. Yu, X. Chen, C. Zhong, D. W. K. Ng and Z. Zhang, "Design, Analysis and Optimization of A Large Intelligent Reflecting Surface Aided B5G Cellular Internet of Things," in *IEEE Internet of Things Journal*.
35. X. Liang, Y. Wu, D. W. K. Ng, S. Jin, Y. Yao and T. Hong, "Outage Probability of Cooperative NOMA Networks Under Imperfect CSI With User Selection," in *IEEE Access*, vol. 8, pp. 117921-117931, 2020.
36. W. Yuan, Z. Wei, J. Yuan and D. W. K. Ng, "A Simple Variational Bayes Detector for Orthogonal Time Frequency Space (OTFS) Modulation," in *IEEE Transactions on Vehicular Technology*, vol. 69, no. 7, pp. 7976-7980, July 2020.
37. W. Yuan, S. Li, L. Xiang and D. W. K. Ng, "Distributed Estimation Framework for Beyond 5G Intelligent Vehicular Networks," in *IEEE Open Journal of Vehicular Technology*, vol. 1, pp. 190-214, 2020.
38. W. Wang *et al.*, "Energy-Constrained UAV-Assisted Secure Communications With Position Optimization and Cooperative

Jamming," in *IEEE Transactions on Communications*, vol. 68, no. 7, pp. 4476-4489, July 2020.

39. R. Li, Z. Wei, L. Yang, D. W. K. Ng, J. Yuan and J. An, "Resource Allocation for Secure Multi-UAV Communication Systems With Multi-Eavesdropper," in *IEEE Transactions on Communications*, vol. 68, no. 7, pp. 4490-4506, July 2020.
40. Y. Cai, Z. Wei, R. Li, D. W. K. Ng and J. Yuan, "Joint Trajectory and Resource Allocation Design for Energy-Efficient Secure UAV Communication Systems," in *IEEE Transactions on Communications*, vol. 68, no. 7, pp. 4536-4553, July 2020.
41. Y. Zhou, F. Zhou, H. Zhou, D. W. K. Ng and R. Q. Hu, "Robust Trajectory and Transmit Power Optimization for Secure UAV-Enabled Cognitive Radio Networks," in *IEEE Transactions on Communications*, vol. 68, no. 7, pp. 4022-4034, July 2020.
42. K. Wang, Q. Wu, W. Chen, Y. Yang and D. W. K. Ng, "Energy-Efficient Buffer-Aided Relaying Systems with Opportunistic Spectrum Access," in *IEEE Transactions on Green Communications and Networking*.
43. W. Yuan, N. Wu, Q. Guo, D. W. K. Ng, J. Yuan and L. Hanzo, "Iterative Joint Channel Estimation, User Activity Tracking, and Data Detection for FTN-NOMA Systems Supporting Random Access," in *IEEE Transactions on Communications*, vol. 68, no. 5, pp. 2963-2977, May 2020.
44. T. Zheng, H. Wang, D. W. K. Ng and J. Yuan, "Physical-Layer Security in the Finite Blocklength Regime Over Fading Channels," in *IEEE Transactions on Wireless Communications*, vol. 19, no. 5, pp. 3405-3420, May 2020.

45. P. Zhang, J. Zhang, K. P. Peppas, D. W. K. Ng and B. Ai, "Dual-Hop Relaying Communications Over Fisher-Snedecor F-Fading Channels," in *IEEE Transactions on Communications*, vol. 68, no. 5, pp. 2695-2710, May 2020.
46. A. Khalili, S. Akhlaghi, H. Tabassum and D. W. K. Ng, "Joint User Association and Resource Allocation in the Uplink of Heterogeneous Networks," in *IEEE Wireless Communications Letters*, vol. 9, no. 6, pp. 804-808, June 2020.
47. D. Xu, Y. Sun, D. W. K. Ng and R. Schober, "Multiuser MISO UAV Communications in Uncertain Environments With No-Fly Zones: Robust Trajectory and Resource Allocation Design," in *IEEE Transactions on Communications*, vol. 68, no. 5, pp. 3153-3172, May 2020.
48. C. Ouyang, S. Wu, C. Jiang, D. W. K. Ng and H. Yang, "Receive Antenna Selection Under Discrete Inputs: Approximation and Applications," in *IEEE Transactions on Communications*, vol. 68, no. 4, pp. 2634-2647, April 2020.
49. Q. Qi, X. Chen and D. W. K. Ng, "Robust Beamforming for NOMA-Based Cellular Massive IoT With SWIPT," in *IEEE Transactions on Signal Processing*, vol. 68, pp. 211-224, 2020.
50. J. Xu, W. Xu, D. W. K. Ng and A. L. Swindlehurst, "Secure Communication for Spatially Sparse Millimeter-Wave Massive MIMO Channels via Hybrid Precoding," in *IEEE Transactions on Communications*, vol. 68, no. 2, pp. 887-901, Feb. 2020.
51. R. Morsi, V. Jamali, A. Hagelauer, D. W. K. Ng and R. Schober, "Conditional Capacity and Transmit Signal Design for SWIPT Systems With Multiple Nonlinear Energy Harvesting Receivers," in *IEEE Transactions on Communications*, vol. 68, no. 1, pp. 582-601, Jan. 2020.

52. Z. Wei, L. Yang, D. W. K. Ng, J. Yuan and L. Hanzo, "On the Performance Gain of NOMA Over OMA in Uplink Communication Systems," in *IEEE Transactions on Communications*, vol. 68, no. 1, pp. 536-568, Jan. 2020.
53. A. Khalili, M. Robat Mili, M. Rasti, S. Parsaeefard and D. W. K. Ng, "Antenna Selection Strategy for Energy Efficiency Maximization in Uplink OFDMA Networks: A Multi-Objective Approach," in *IEEE Transactions on Wireless Communications*, vol. 19, no. 1, pp. 595-609, Jan. 2020.
54. D. Xu, X. Yu, Y. Sun, D. W. K. Ng and R. Schober, "Resource Allocation for Secure IRS-Assisted Multiuser MISO Systems," *2019 IEEE Globecom Workshops (GC Wkshps)*, Waikoloa, HI, USA, 2019, pp. 1-6.
55. J. Liu, K. Xiong, D. W. K. Ng, P. Fan and Z. Zhong, "Optimal Design of Wireless-Powered Hierarchical Fog-Cloud Computing Networks," *2019 IEEE Global Communications Conference (GLOBECOM)*, Waikoloa, HI, USA, 2019, pp. 1-6.
56. Y. Cai, Z. Wei, R. Li, D. W. Kwan Ng and J. Yuan, "Energy-Efficient Resource Allocation for Secure UAV Communication Systems," *2019 IEEE Wireless Communications and Networking Conference (WCNC)*, Marrakesh, Morocco, 2019, pp. 1-8.
57. B. Feng *et al*., "Joint Millimeter Wave and Microwave Wave Resource Allocation Design for Dual-Mode Base Stations," *2019 IEEE Wireless Communications and Networking Conference (WCNC)*, Marrakesh, Morocco, 2019, pp. 1-6.
58. X. Sun, D. W. K. Ng, Z. Ding, Y. Xu and Z. Zhong, "Physical Layer Security in UAV Systems: Challenges and Opportunities," in *IEEE Wireless Communications*, vol. 26, no. 5, pp. 40-47, October 2019.

59. Z. Wei, S. Sun, X. Zhu, D. In Kim and D. W. K. Ng, "Resource Allocation for Wireless-Powered Full-Duplex Relaying Systems With Nonlinear Energy Harvesting Efficiency," in *IEEE Transactions on Vehicular Technology*, vol. 68, no. 12, pp. 12079-12093, Dec. 2019.
60. Q. Qi, X. Chen, D. W. K. Ng, C. Zhong and Z. Zhang, "Robust Beamforming Design for SWIPT in Cellular Internet of Things," *2019 IEEE/CIC International Conference on Communications in China (ICCC)*, Changchun, China, 2019, pp. 523-528.
61. M. Najafi, V. Jamali, D. W. K. Ng and R. Schober, "C-RAN With Hybrid RF/FSO Fronthaul Links: Joint Optimization of Fronthaul Compression and RF Time Allocation," in *IEEE Transactions on Communications*, vol. 67, no. 12, pp. 8678-8695, Dec. 2019.
62. Z. Wei, M. Qiu, D. W. Kwan Ng and J. Yuan, "A Two-Stage Beam Alignment Framework for Hybrid MmWave Distributed Antenna Systems," *2019 IEEE 20th International Workshop on Signal Processing Advances in Wireless Communications (SPAWC)*, Cannes, France, 2019, pp. 1-5.
63. G. Yu, X. Chen and D. W. K. Ng, "Low-Cost Design of Massive Access for Cellular Internet of Things," in *IEEE Transactions on Communications*, vol. 67, no. 11, pp. 8008-8020, Nov. 2019.
64. L. Zhao, J. Guo, Z. Wei, D. W. K. Ng and J. Yuan, "A Distributed Multi-RF Chain Hybrid mmWave Scheme for Small-Cell Systems," *ICC 2019 - 2019 IEEE International Conference on Communications (ICC)*, Shanghai, China, 2019, pp. 1-7
65. Z. Wei, D. W. K. Ng and J. Yuan, "Beamwidth Control for NOMA in Hybrid mmWave Communication Systems," *ICC 2019 - 2019 IEEE International Conference on Communications (ICC)*, Shanghai, China, 2019, pp. 1-6.

66. R. Jia, X. Chen, D. W. K. Ng, H. Lin and Z. Zhang, "Design of Beamspace Massive Access for Cellular Internet-of-Things," *ICC 2019 - 2019 IEEE International Conference on Communications (ICC)*, Shanghai, China, 2019, pp. 1-7.
67. X. Li, X. Zhou, D. W. K. Ng and C. Sun, "Optimal Online Transmission Policy for Energy-Constrained Wireless-Powered Communication Networks," *ICC 2019 - 2019 IEEE International Conference on Communications (ICC)*, Shanghai, China, 2019, pp. 1-7.
68. X. Sun, C. Shen, D. W. K. Ng and Z. Zhong, "Robust Trajectory and Resource Allocation Design for Secure UAV-Aided Communications," *2019 IEEE International Conference on Communications Workshops (ICC Workshops)*, Shanghai, China, 2019, pp. 1-6.
69. S. Hu, Z. Wei, Y. Cai, D. W. K. Ng and J. Yuan, " Sum-Rate Maximization for Multiuser MISO Downlink Systems with Self-sustainable IRS," *[URL]:* https://arxiv.org/abs/2005.11663, *2020.*